

1 **Interleukin-3 is a predictive marker for severity and outcome during SARS-CoV-2**  
2 **infections**  
3

4 Alan Bénard<sup>1\*</sup>, Anne Jacobsen<sup>1</sup>, Maximilian Brunner<sup>1</sup>, Christian Krautz<sup>1</sup>, Bettina Klösch<sup>1</sup>,  
5 Izabela Swierzy<sup>1</sup>, Elisabeth Naschberger<sup>1</sup>, Torsten Birkholz<sup>2</sup>, Ixchel Castellanos<sup>2</sup>, Denis  
6 Trufa<sup>3</sup>, Horia Sirbu<sup>3</sup>, Marcel Vetter<sup>4</sup>, Andreas E. Kremer<sup>4</sup>, Kai Hildner<sup>4</sup>, Andreas Hecker<sup>5</sup>,  
7 Fabian Edinger<sup>5</sup>, Matthias Tenbusch<sup>6</sup>, Enrico Richter<sup>7</sup>, Hendrik Streeck<sup>7</sup>, Marc M. Berger<sup>8</sup>,  
8 Thorsten Brenner<sup>8</sup>, Markus A. Weigand<sup>9</sup>, Filip K. Swirski<sup>10</sup>, Georg Schett<sup>11</sup>, Robert  
9 Grützmann<sup>1</sup>, and Georg F. Weber<sup>1\*</sup>

10  
11 <sup>1</sup> Department of Surgery, Friedrich-Alexander University (FAU) Erlangen-Nürnberg and  
12 Universitätsklinikum Erlangen, Erlangen, Germany

13 <sup>2</sup> Department of Anesthesiology, Friedrich-Alexander University (FAU) Erlangen-  
14 Nürnberg and Universitätsklinikum Erlangen, Erlangen, Germany

15 <sup>3</sup> Department of Thoracic Surgery, Friedrich-Alexander University (FAU) Erlangen-  
16 Nürnberg and Universitätsklinikum Erlangen, Erlangen, Germany

17 <sup>4</sup> Department of Internal Medicine 1 - Gastroenterology, Pneumology and Endocrinology,  
18 Friedrich-Alexander University (FAU) Erlangen-Nürnberg and Universitätsklinikum  
19 Erlangen, Erlangen, German

20 <sup>5</sup> Department of Surgery, University Hospital, Giessen, Germany

21 <sup>6</sup> Institute of Clinical and Molecular Virology, Friedrich-Alexander University (FAU)  
22 Erlangen-Nürnberg and Universitätsklinikum Erlangen, Erlangen, Germany

23 <sup>7</sup> Institute of Virology, University Hospital, Bonn, Germany

24 <sup>8</sup> Department of Anesthesiology and Intensive Care Medicine, Essen University Hospital,  
25 Essen, Germany

26 <sup>9</sup> Department of Anesthesiology, Heidelberg University Hospital, Heidelberg, Germany

27 <sup>10</sup> Center for Systems Biology, Massachusetts General Hospital and Harvard Medical School,  
28 Boston, MA, USA

29 <sup>11</sup> Department of Internal Medicine 3 - Rheumatology and Immunology, Friedrich-Alexander  
30 University (FAU) Erlangen-Nürnberg and Universitätsklinikum Erlangen, Erlangen,  
31 Germany

32  
33 \* Corresponding authors: Georg F. Weber; Alan Bénard

34  
35 Correspondence to:

36 Georg F. Weber

37 Email: [georg.weber@uk-erlangen.de](mailto:georg.weber@uk-erlangen.de)

38 Phone: +49-9131-85-42046

39

40 Or

41

42 Alan Bénard

43 Email: [alan.benard@uk-erlangen.de](mailto:alan.benard@uk-erlangen.de)

44 Phone: +49-9131-85-42055

45

46 Department of Surgery

47 Universitätsklinikum Erlangen

48 Friedrich-Alexander University (FAU) Erlangen-Nürnberg

49 Erlangen

50 Germany

51 **Abstract**

52 Severe acute respiratory syndrome coronavirus 2 (SARS-CoV-2) is a worldwide health threat.

53 Here, we report that low plasma interleukin-3 (IL-3) levels were associated with increased

54 severity and mortality during SARS-CoV-2 infections. IL-3 promoted the recruitment of

55 antiviral circulating plasmacytoid dendritic cells (pDCs) into the airways by stimulating

56 CXCL12 secretion from pulmonary CD123<sup>+</sup> epithelial cells. This study identifies IL-3 as a

57 predictive disease marker and potential therapeutic target for SARS-CoV-2 infections.

58

59

60

61

62

63

64

65

66

67

68

69

70

71

72

73

74

75

76

## 77 **Main Text**

78           Coronavirus Disease 2019 (COVID-19) is an acute infection of the respiratory tract  
79 that had spread worldwide<sup>1</sup>. As patients may develop severe respiratory syndrome<sup>2</sup>, it is  
80 important to define predictive markers allowing clinicians to identify patients at risk at an  
81 early stage of the disease. IL-3 has been described as an important immune mediator during  
82 infections<sup>3,4</sup>. We therefore investigated whether IL-3 might influence the outcome of SARS-  
83 CoV-2 infection.

84           Patients with severe COVID-19, characterized by necessity for intensive care  
85 treatment and high plasma CRP levels (Extended Data Fig. 1a), had reduced plasma IL-3  
86 levels as compared to patients with non-severe COVID-19 or patients that had recovered (Fig.  
87 1a). As well, patients with high viral load presented lower plasma IL-3 levels as compared to  
88 patients with low viral load (Fig. 1b), both results suggesting an association between plasma  
89 IL-3 levels and disease severity in SARS-CoV-2 infections. In this prospective multicentric  
90 observation study, Kaplan-Meier survival analysis revealed that plasma IL-3 levels may  
91 predict the outcome of SARS-CoV-2 infections: using a minimal p-value approach, patients  
92 with plasma IL-3 levels <20 pg/ml at admission had a poorer prognosis as compared to  
93 patients with plasma IL-3 levels  $\geq$ 20 pg/ml at admission (Fig. 1c and Extended Data Table 1),  
94 this association remaining significant after adjusting for prognostic parameters in multivariate  
95 analysis (Extended Data Table 2). Older age was described to be associated with greater risk  
96 to develop severe COVID-19<sup>5</sup>. Patients older than 65 years showed reduced plasma IL-3  
97 levels as compared to patients younger than 65 years (Fig. 1d). Thus, the analysis of plasma  
98 IL-3 levels and patient age allowed to identify three groups at risk to die from COVID-19:  
99 patients <65 years with plasma IL-3 levels  $\geq$ 20 or <20 pg/ml had a low to intermediate risk to  
100 die whereas patients  $\geq$ 65 years with plasma IL-3 levels <20 pg/ml had a high risk to die (95%-  
101 CI: 1.680 – 118.218; OR: 14.091) (Fig. 1e, Extended Data Fig. 1b and Extended Data Table  
102 3). Survivors from severe SARS-CoV-2 infection displayed higher circulating pDC numbers

103 over time as compared to non-survivors whereas no differences could be detected in the  
104 numbers of circulating neutrophils (Fig. 1f). SARS-CoV-2<sup>+</sup> patients exhibiting either high  
105 plasma IL-3 levels or high circulating pDC numbers had therefore a better prognosis,  
106 suggesting a putative link between IL-3 and pDCs during infection. Bronchoalveolar lavage  
107 fluid (BALF) analysis (Extended Data Table 4) revealed that patients with high levels of IL-3  
108 showed increased percentages of pDCs as compared to those with low levels (Fig. 1g).

109 We next investigated the link between IL-3 and the amount of pDCs in the airways  
110 experimentally. Upon intranasal (i.n.) IL-3 administration, naive WT mice displayed higher  
111 absolute numbers of pDCs, but not neutrophils, in the lung parenchyma as compared to  
112 controls (Fig. 2a and Extended Data Fig. 2a) as well as substantially higher levels of IFN $\alpha$  and  
113 IFN $\lambda$  in the BALF after subsequent i.n. CpG injection (Fig. 2b). Depletion of pDCs induced a  
114 strong reduction of IFN $\alpha$  levels in BALF of mice pre-treated with IL-3 upon i.n. CpG  
115 administration, whereas IFN $\lambda$  secretion was only partially impaired (Extended Data Fig. 2b-  
116 c). Among the chemokines known to drive pDC migration into inflamed tissues<sup>6</sup>, only *Cxcl12*  
117 expression was increased by IL-3 treatment in lungs of mice upon CpG administration (Fig.  
118 2c and Extended Data Fig. 3a). We also detected increased CXCL12 levels in the BALF of  
119 WT mice treated with IL-3 (Fig. 2d) and in the supernatant of *ex vivo* cultured lung cells  
120 derived from naive WT mice upon IL-3 stimulation (Extended Data Fig. 3b). The induction of  
121 CXCL12 was mediated through the IL-3 receptor common  $\beta$ -chain (CD131), as no increase in  
122 CXCL12 levels was observed in the BALF of *Cd131*<sup>-/-</sup> mice upon IL-3 stimulation (Fig. 2d).  
123 I.n. injection of CXCL12 in mice resulted in increased numbers of pDCs but not neutrophils  
124 in the lungs (Extended Data Fig. 3c). Additionally, i.n. injection of CXCL12-neutralizing  
125 antibodies prevented pDC influx into the lungs of WT mice upon IL-3 injection, whereas no  
126 difference was observed for neutrophils (Fig. 2f). In SARS-CoV-2<sup>+</sup> patients, plasma IL-3  
127 levels strongly correlated with plasma CXCL12 levels, but not with plasma IL-6, TNF and  
128 CRP levels (Fig. 2g and Extended Data Fig. 4a-c). CXCL12 plasma levels were also not

129 correlated with circulating pDC number (Extended Data Fig. 4d). In BALF of patients with  
130 different respiratory diseases, IL-3 positively correlated with CXCL12 levels (Fig. 2h) and  
131 high levels of CXCL12 were associated with increased percentages of pDCs (Fig. 2i).

132 We found that only CD45<sup>-</sup> non-haematopoietic cells expressed the  $\alpha$ -chain of the IL-3  
133 receptor (CD123) in the lungs of naive mice (Extended Data Fig. 5a). Likewise, only CD45<sup>-</sup>  
134 cells secreted CXCL12 after IL-3 stimulation (Extended Data Fig. 5b). Flow cytometry  
135 analyses revealed that only epithelial cells were found to overexpress CXCL12 in the lungs of  
136 mice upon *ex vivo* IL-3 stimulation (Extended Data Fig. 5c). As well, CXCL12 was only  
137 expressed by CD326<sup>+</sup> CD123<sup>+</sup> epithelial cells in human lungs (Fig 2j-k and Extended Data  
138 Table 5).

139 Collectively, our study revealed that plasma IL-3 levels might allow risk stratification  
140 in patients with SARS-CoV-2 infections. We therefore propose IL-3 as a predictive marker  
141 for disease severity and clinical outcome. Based on its ability to improve local antiviral  
142 defence mechanisms by recruiting pDCs, recombinant IL-3, or CD123 receptor agonists, may  
143 therefore have the potential as novel therapeutic agents in SARS-CoV-2 infected patients.

144

145

146

147

148

149

150

151 **References**

- 152 1. Zhu, N., *et al.* A Novel Coronavirus from Patients with Pneumonia in China, 2019.  
153 *The New England journal of medicine* **382**, 727-733 (2020).
- 154 2. Huang, C., *et al.* Clinical features of patients infected with 2019 novel coronavirus in  
155 Wuhan, China. *Lancet* **395**, 497-506 (2020).
- 156 3. Weber, G.F., *et al.* Interleukin-3 amplifies acute inflammation and is a potential  
157 therapeutic target in sepsis. *Science* **347**, 1260-1265 (2015).
- 158 4. Auclair, S.R., *et al.* Interleukin-3-deficient mice have increased resistance to blood-  
159 stage malaria. *Infection and immunity* **82**, 1308-1314 (2014).
- 160 5. Wu, C., *et al.* Risk Factors Associated With Acute Respiratory Distress Syndrome and  
161 Death in Patients With Coronavirus Disease 2019 Pneumonia in Wuhan, China. *JAMA*  
162 *internal medicine* (2020).
- 163 6. Swiecki, M. & Colonna, M. The multifaceted biology of plasmacytoid dendritic cells.  
164 *Nature reviews. Immunology* **15**, 471-485 (2015).

165

166

167

168

169

170

171

172

173

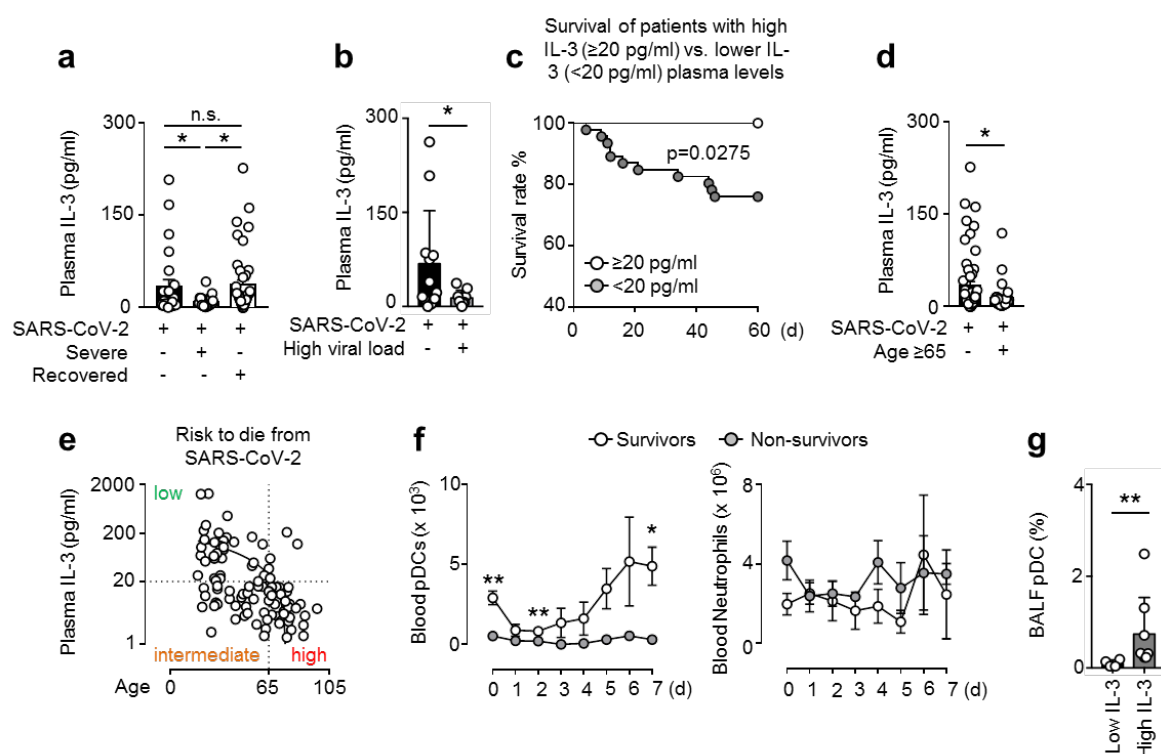
174

175

176

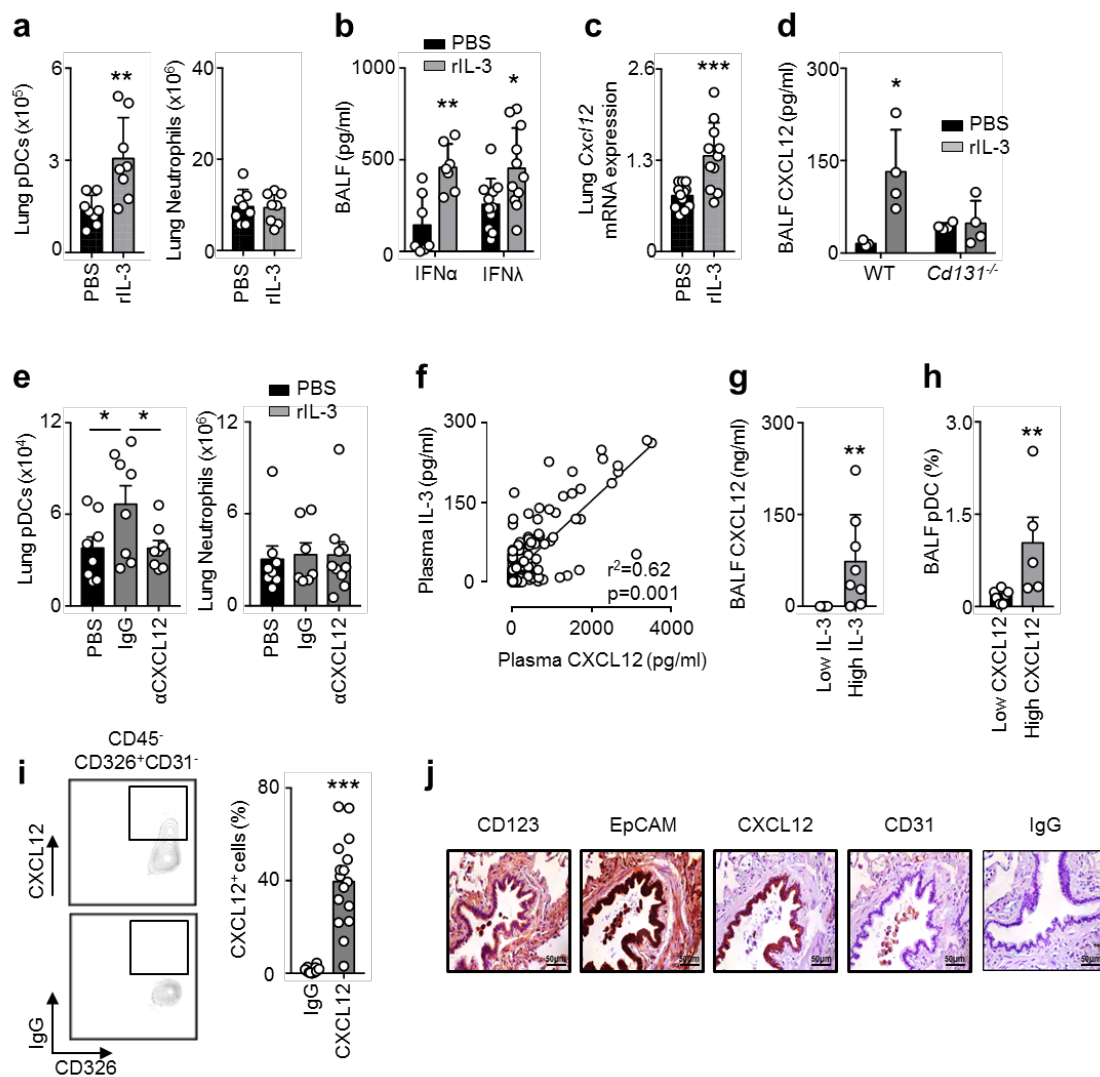
177

178 **Figures**



179

180 **Figure 1. Low plasma interleukin-3 levels are associated with severity and outcome in**  
 181 **COVID-19. a,** Plasma IL-3 levels of SARS-CoV-2<sup>+</sup> patients with or without severe disease  
 182 and in patients that had recovered from infection. One-way ANOVA. n=106. **b,** Plasma IL-3  
 183 levels of SARS-CoV-2<sup>+</sup> patients with or without high viral load. n=21. **c,** Kaplan-Meier  
 184 analysis showing the survival of SARS-CoV-2<sup>+</sup> patients with high ( $\geq 20$ pg/ml) or low  
 185 ( $< 20$ pg/ml) plasma IL-3 levels (measured within 24 hrs after admission). n=64. **d,** Plasma IL-  
 186 3 levels of SARS-CoV-2<sup>+</sup> patients older or younger than 65 years. n=106. **e,** Correlation  
 187 between plasma IL-3 levels and age. n=106. **f,** Absolute numbers of circulating pDCs and  
 188 neutrophils in SARS-CoV-2<sup>+</sup> patients from their admission to ICU and 1 to 7 days later. n=9.  
 189 **g,** Percentage of pDCs in BALF of patients with pulmonary diseases with high or low BALF  
 190 IL-3 levels. n=13. Data are mean  $\pm$  s.e.m., \*P < 0.05, \*\*P < 0.01, \*\*\*P < 0.001, unpaired, 2-  
 191 tailed Student's t test using Welch's correction for unequal variances was used.



192

193 **Figure 2. Interleukin-3 promotes the recruitment of pDCs into the lung in a CXCL12-**  
 194 **dependent manner.** **a**, Absolute numbers of pDCs and neutrophils in the lungs of naive mice  
 195 24 h after the i.n. injection of PBS or IL-3. n=8. **b**, Levels of IFN $\alpha$  and IFN $\lambda$  in the BALF of  
 196 naive mice that received an i.n. injection of PBS or IL-3, followed by an i.n. injection of CpG  
 197 8 h later, and were sacrificed 16 h later. n=7-11. **c**, Relative mRNA expression of *Cxcl12* in  
 198 the lungs of naive mice 24 h after the i.n. injection of PBS or IL-3. n=12. **d**, Level of CXCL12  
 199 in the BALF of WT or *Cd131*<sup>-/-</sup> mice 24 h after the i.n. injection of PBS or IL-3. n=4-5. **e**,  
 200 Absolute number of pDCs and neutrophils in the lungs of naive mice 24 h after the i.n.  
 201 injection of PBS, IgG or anti-CXCL12 in combination with the i.n. injection of PBS (black)  
 202 or IL-3 (grey). n=8. **f**, Correlation between plasma IL-3 and CXCL12 levels of SARS-CoV-2<sup>+</sup>



203 patients. n=106. **g**, Level of CXCL12 in the BALF of patients with pulmonary diseases with  
204 high or low IL-3 BALF levels. n=13. **h**, Percentage of pDCs in the BALF of patients with  
205 pulmonary diseases with high or low CXCL12 BALF levels. n=13. **i**, Percentage of CXCL12<sup>+</sup>  
206 epithelial cells in the lungs of patients with pulmonary inflammation. n=15. **j**,  
207 Immunohistochemistry of EpCAM, CXCL12, CD31, and IgG in the lungs of patients with  
208 pulmonary inflammation. Data are mean  $\pm$  s.e.m., \*P < 0.05, \*\*P < 0.01, \*\*\*P < 0.001,  
209 unpaired or Mann Whitney test were used.

210

211

212

213

214

215

216

217

218

219

220

221

222

223

224 **Supplemental Information**

225

226 **Materials & Methods**

227 **Animals:** Balb/c (WT), C57Bl/6J (WT) (Janvier, Le Genest-Saint-Isle, France) and *Cd131*<sup>-/-</sup>  
228 (C57Bl/6J background, bred in-house) mice were used in this study. Majority of the mice  
229 were 8-12 weeks old when sacrificed. All animal protocols were approved by the animal  
230 review committee from the university hospital Dresden and Erlangen and the local  
231 governmental animal committee.

232

233 **Mouse infection:** Naive mice were anesthetized with isoflurane and infected intra-nasally  
234 with 8µg of CpG (Enzo Life Sciences, Farmingdale, NY, USA), 400ng of recombinant IL-3  
235 (R&D Systems, Minneapolis, MN, USA), 500ng of recombinant CXCL12 (Peprotech, Rocky  
236 Hill, NJ, USA), 50µg of IgG or anti-CXCL12 (R&D systems). For the pDCs depletion  
237 experiment, 150µg of IgG or anti-CD317 (Miltenyi) were injected intravenously 15h hour  
238 before IL-3 and CpG injection.

239

240 **Murine leukocytes isolation:** After lungs harvest, single cell suspensions were obtained as  
241 follows: perfused lungs were cut in small pieces and subjected to enzymatic digestion with  
242 450 U/ml collagenase I (Sigma Aldrich), 125 U/ml collagenase IX (Sigma Adrich), 60 U/ml  
243 hyaluronidase (Sigma Aldrich), 60 U/ml Dnase (Sigma Aldrich) and 20 mM Hepes (Thermo  
244 Fisher Scientific, Waltham, MA, USA) for 1 hour at 37°C while shaking. Broncho-alveolar  
245 lavage (BAL) was performed by flushing the lungs with 2 × 1 ml of PBS to retrieve the  
246 infiltrated and resident leukocytes. Total viable cell numbers were obtained using Trypan Blue  
247 (Carl Roth).

248 **Quantitative RT-PCR:** Real-time PCR was performed as previously described<sup>1</sup>. Briefly,  
249 RNA was extracted from whole tissue by RNeasy mini kit (Qiagen, Venlo, Netherlands).  
250 Complementary DNA was reverse transcribed from 1 µg total RNA with Moloney murine  
251 leukemia virus reverse transcriptase (Thermo Fisher Scientific) using random hexamer  
252 oligonucleotides for priming (Thermo Fisher Scientific). The amplification was performed  
253 with a Biorad CFX-Connect Real-time-System (Thermo Fisher Scientific) using the SYBR  
254 Green (Eurogentec, Seraing, Belgium) or TaqMan (Thermo Fisher Scientific) detection  
255 system. Data were analyzed using the software supplied with the Sequence Detector (Life  
256 Technologies). The mRNA content for *Cxcl12*, *Ccl2*, *Cxcl9* and *Ccl21* was normalized to the  
257 hypoxanthine-guanine phosphoribosyltransferase (*Hprt*) mRNA for mouse genes. Gene  
258 expression was quantified using the  $\Delta\Delta C_t$  method. The expression level was arbitrarily set to  
259 1 for one sample from the PBS group, and the values for the other samples were calculated  
260 relatively to this reference. The sequence of primers is in Extended Data Table 3.

261  
262 **Cytokine detection:** Mouse: Secreted CXCL12 (R&D systems), IFN $\lambda$  (R&D systems) and  
263 IFN $\alpha$  (R&D systems) were measured by ELISA according to the manufacturer's instructions.  
264 Human: Secreted CXCL12 (R&D Systems), IL-3 (R&D Systems), IL-6 (Biolegend) and TNF  
265 (Biolegend) were measured by ELISA according to the manufacturer's instructions.

266  
267 **Lung cells stimulation *in vitro*:** Lung cell suspensions from naive mice were cultured in  
268 RPMI-1640 GlutaMax supplemented with 10% FCS, 25mM of HEPES, 1 mM sodium  
269 pyruvate, 100U/ml of Penicillin-Streptomycin and 20µg/ml of Gentamicin at 37°C in the  
270 presence of 5% CO<sub>2</sub>. Lung cell suspensions were stimulated in 12-well plates (10<sup>6</sup> cells/ml)  
271 during 24h by IL-3 (20ng/ml). Then supernatants were collected for cytokine measurement.

272 CD45<sup>-</sup> and CD45<sup>+</sup> cells were purified from lungs of naive mice using CD45 microbeads  
273 (Miltenyi Biotec), according to the manufacturer's instructions.

274

275 **Immunohistochemistry:** For CXCL12 and EpCAM permanent immunohistochemistry, the  
276 staining was performed as previously described<sup>2</sup>. The characteristics of the respective patients  
277 are detailed in Extended Data Table 2. In brief, formalin-fixed, paraffin-embedded lung  
278 tissues were deparaffinized by xylene two times for 15 min. The tissue was rehydrated using  
279 decreasing concentrations of ethanol (100%, 96%, 85% and 70%) for 2 min each. Antigen  
280 retrieval was performed using Target Retrieval Solution (DakoCytomation) at pH 9.0 at 95°C  
281 for 20 min followed by cooling for 20 min at RT. As a washing buffer between the incubation  
282 steps, 1xTBS pH 7.6 was used. The slides were blocked by hydrogen peroxide (7.5%, Sigma-  
283 Aldrich), avidin-biotin-block (Vector Laboratories, Burlingame, CA, USA) and 10% donkey  
284 normal serum (DNS, Vector Laboratories) in TBS for 10 min. The primary antibodies diluted  
285 in 2.5% DNS (rabbit anti-human EpCAM cat no. ab71916, Abcam, 1:300; mouse anti-human  
286 CXCL12 cat. no. MAB350, R&D Systems, 1:150) and isotype control antibodies in  
287 corresponding concentrations were detected using either the RTU Vectastain Elite ABC Kit  
288 anti-mouse/rabbit (for EpCAM and CXCL12; Vector Laboratories) and NovaRed substrate  
289 (Vector Laboratories) as a substrate. The slides were counterstained with Gill-III hematoxylin  
290 (Merck), dehydrated and mounted with VectaMount permanent mounting medium (Vector  
291 Laboratories). The sections were analyzed using a DM6000 B microscope (Leica).

292

293 **Flow Cytometry:** The following antibodies were used for flow cytometric analyses: Mouse:  
294 anti-CD317-BV650 (Biolegend), anti-Ly6C-FITC (BD Biosciences), anti-B220-BUV737 (BD  
295 Biosciences), anti-CD11c-PerCP Cy5.5 (Biolegend), anti-CD11b-PE CF594 (BD  
296 Biosciences), anti-F4/80-BV510 (BD Biosciences), anti-Ly6G-BUV395 (BD Biosciences),

297 anti-SiglecH-Pacific Blue (BD Biosciences), anti-CD45.2-BV786 (BD Biosciences), anti-  
298 MHCII-BV711 (BD Biosciences), anti-CD19-BV421 (BD Biosciences), anti-CD3- PerCP  
299 Cy5.5 (Biolegend), IgG2a-PE (Biolegend), anti-CD146-FITC (Biolegend), anti-CD31-Pacific  
300 Blue (Biolegend), anti-CD326-PE-CF594 (Biolegend), anti-CD326-BV650 (BD Biosciences),  
301 anti-CD123-PE (Biolegend). Human: anti-CD45-Pacific Blue (Biolegend), anti-CD45-BV786  
302 (BD Biosciences), anti-CD303-PerCP Cy5.5 (Biolegend), anti-HLA-DR-BUV395 (BD  
303 Biosciences), anti-CD11c-BV711 (BD Biosciences), anti-CD326-PerCP Cy5.5 (Biolegend),  
304 anti-CD31-BV711 (BD Biosciences), anti-CD14-BUV737 (BD Biosciences), anti-CD16-  
305 BV421 (BD Biosciences), anti-CD11b-BV711 (BD Biosciences), anti-CD15-PE (BD  
306 Biosciences). Anti-CXC12-PE (R&D Systems) and IgG1-PE (R&D Systems) were used for  
307 mouse and human. Staining for intracellular cytokines was performed using BD  
308 Cytotfix/Cytoperm Plus Kit (BD Biosciences). Data were acquired on a Celesta (BD  
309 Biosciences) flow cytometer and analyzed with FlowJo 10 (FlowJo LLC, Ashland, OR,  
310 USA).

311

312 **Human specimen:** This prospective, multicentric, observational clinical study was first  
313 approved by the local ethics committee on February, 1<sup>st</sup> 2016 (UKER 10\_16 B), and modified  
314 on April, 28<sup>th</sup> 2020 (UKER 174\_20 B). Departments from 3 additional University Hospitals in  
315 Germany participated in this study. Prospective measurements of Interleukin-3 and analysis of  
316 patients participating in the trial have been conducted between April 1<sup>st</sup> 2020 and June 4<sup>th</sup>  
317 2020. The observational clinical studies were conducted in the medical wards and intensive  
318 care units of the (i) University Hospital of Erlangen, Germany; (ii) University Hospital of  
319 Essen, Germany; (iii) University Hospital of Giessen, Germany; and (iv) University Hospital  
320 of Bonn, Germany. Study patients or their legal designees signed written informed consent. In  
321 total, 106 (32 non-severe; 32 severe; 42 recovered) patients positive for SARS-CoV-2 PCR

322 from oral swabs, oral fluid, or bronchoalveolar lavage fluid were enrolled in this trial. Blood  
323 samples were collected at the onset of symptoms ( $\leq 24$  hours), and 1, 2, 3, 4, 5, 6, or 7 days  
324 later; or after recovery from SARS-CoV-2 infection. Patients with high viral load are patients  
325 with CT levels above the median of all patients (Median CT levels: 32.63). 20 healthy donors  
326 served as controls. *Blood*: After blood collection, plasma of all study participants was  
327 immediately obtained by centrifugation, transferred into cryotubes, and stored at  $-80^{\circ}\text{C}$  until  
328 further processing. For flow cytometry analysis, red blood cells were removed by centrifuging  
329 blood cells 7 min at 400g without break in Leukosep tube (Greiner, Kremsmünster, Austria).  
330 Leukocytes were then stained 20 min at  $4^{\circ}\text{C}$  in dark and fixed 1 hour with BD Cytotfix buffer  
331 (BD Biosciences). *Bronchoalveolar-lavage fluid specimen (13 patients)*: After written  
332 informed consent and in agreement with the local ethics review board of the University of  
333 Erlangen (UKER no. 4147) the segmental bronchi of patients scheduled for fiber-optic  
334 bronchoscopy due to various inflammatory and non-inflammatory conditions were flushed  
335 with 100ml sterile 0.9% saline fluid. Fluid has been obtained and processed for flow  
336 cytometric analysis of leukocyte surface markers. In addition, after centrifugation the  
337 supernatants have been stored at  $-80^{\circ}\text{C}$  until further processing. Patients with low IL-3 or low  
338 CXCL12 are patients with a level of IL-3 or CXCL12 under the mean of all the patients.  
339 Patients with high IL-3 or high CXCL12 are patients with a level of IL-3 or CXCL12 above  
340 the mean of all the patients. *Lung tissue specimen (15 patients)*: The study was performed at  
341 the University of Erlangen in Germany. Patients were selected within the framework of the  
342 thoracic surgery board. The patients who underwent surgery and gave their approval were  
343 included in this study. The study was performed in agreement with the local ethics review  
344 board of the University of Erlangen (UKER 10\_16 B, UKER 339\_15 Bc; UKER 56\_12B;  
345 DRKS-ID: DRKS00005376). Patients' confidentiality was maintained. The surgery consisted  
346 of a wedge resection of the lung or lobectomy. Subsequently, tissue samples were taken from  
347 the surgically removed material and transported into the laboratory under standardized

348 conditions (at 4°C, in Ringer's solution) for further preparation and analysis. Samples were  
349 taken from the non-pathological area from the lung for further analysis. For flow cytometry  
350 analysis, separate lung tissue sections were cut into small pieces and subjected to enzymatic  
351 digestion with 450 U/ml collagenase I, 125 U/ml collagenase XI, 60 U/ml DNase I and 60  
352 U/ml hyaluronidase (Sigma-Aldrich, St. Louis, MO) for 1 h at 37°C while shaking at 750 rpm  
353 after which they have been homogenized through a 40µm nylon mesh for flow cytometric  
354 analysis. Total viable cell numbers were obtained using Trypan Blue (Cellgro, Mediatech, Inc,  
355 VA).

356  
357 **Statistics:** Results were expressed as mean ± S.E.M. and expressed as identified in legends.  
358 For comparing 2 groups, statistical tests included unpaired, 2-tailed parametric t tests with  
359 Welch's correction (when Gaussian distribution was assumed), unpaired, 2-tailed  
360 nonparametric Mann-Whitney tests (when Gaussian distribution was not assumed) or paired,  
361 2-tailed parametric t tests. P values of 0.05 or less were considered to denote significance.

362  
363  
364 **Supplemental reference:**

- 365 1. Bénard, A., *et al.* mu-Opioid receptor is induced by IL-13 within lymph nodes from  
366 patients with Sezary syndrome. *Journal of Investigative Dermatology* **130 (5)**, 1337-  
367 44 (2010)
- 368 2. Naschberger, E., *et al.* Matricellular protein SPARCL1 regulates tumor  
369 microenvironment-dependent endothelial cell heterogeneity in colorectal carcinoma.  
370 *Journal of Clinical Investigation* **126 (11)**, 4187-4204

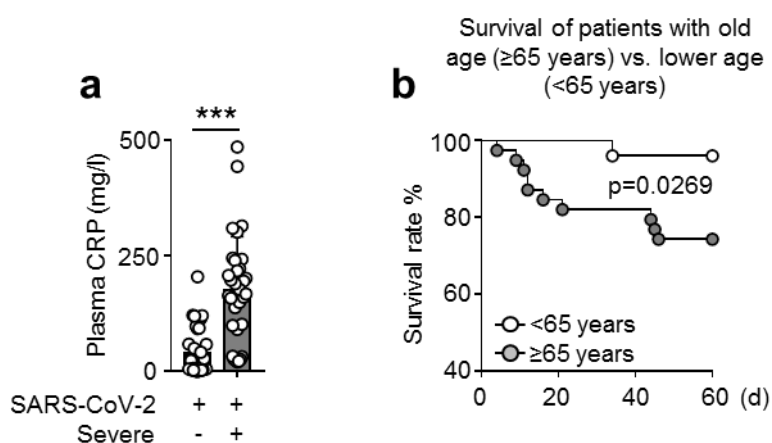
371

372 **Extended Data Figures**

373

374

375



376

377 **Extended Data Fig. 1. Plasma CRP levels and survival of SARS-CoV-2<sup>+</sup> patients with old**

378 **(≥65 years) vs. lower (<65 years) age. a, Plasma CRP levels in SARS-CoV-2<sup>+</sup> patients with**

379 **severe or non-severe disease. Mann Whitney test. n=64. b, Kaplan-Meier analysis showing**

380 **the survival of SARS-CoV-2<sup>+</sup> patients with old (≥65 years) or younger (<65 years) age. n=64.**

381 **Data are mean ± s.e.m., \*P < 0.05, \*\*P < 0.01, \*\*\*P < 0.001.**

382

383

384

385

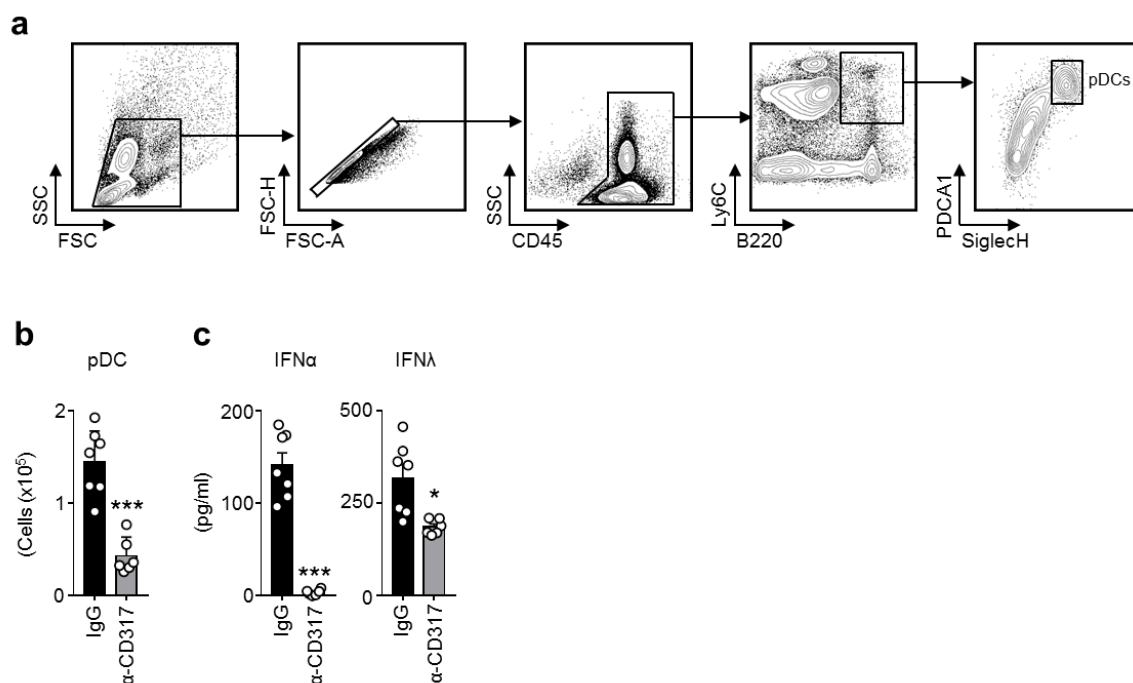
386

387



388

389



390

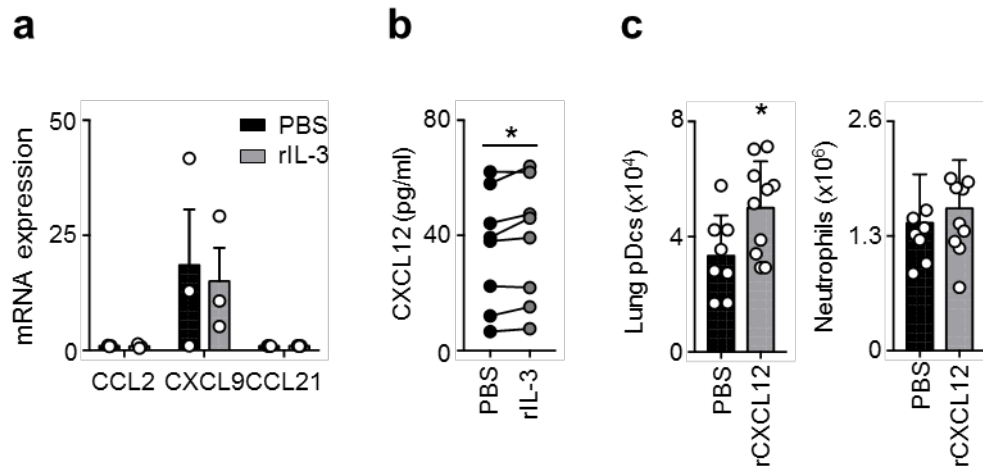
391 **Extended Data Fig. 2. Depletion of pDCs in mice pre-treated with IL-3 induces reduced**  
392 **BALF IFN $\alpha$  and IFN $\lambda$  levels upon i.n. CpG administration. a**, Gating strategy used for  
393 pDCs. **b-c**, Absolute numbers of pDCs in the lungs (**b**) and levels of IFN $\alpha$  and IFN $\lambda$  in the  
394 BALF (**c**) of naive mice intravenously injected with IgG or anti-CD317 15 h before the  
395 injection of IL-3 and CpG. n=7. Data are mean  $\pm$  s.e.m., \*P < 0.05, \*\*P < 0.01, \*\*\*P < 0.001,  
396 unpaired, 2-tailed Student's t test using Welch's correction for unequal variances was used.

397

398

399

400



401

402 **Extended Data Fig. 3. Interleukin-3 induces CXCL12.** a, Relative mRNA expression of

403 *Ccl2*, *Cxcl9* and *Ccl21* in the lungs of naive mice 24 h after the i.n. injection of PBS or IL-3.

404 n=3. b, Levels of CXCL12 in the supernatant of lungs cells from naive mice 24 h after *ex vivo*

405 stimulation with or without IL-3. n=8-14. c, Absolute numbers of pDCs or neutrophils in the

406 lungs of naive mice 24 h after the i.n. injection of PBS or CXCL12. n=7-10. Data are mean  $\pm$

407 s.e.m., \*P < 0.05, \*\*P < 0.01, \*\*\*P < 0.001, paired, 2-tailed Student's t test and unpaired, 2-

408 tailed Student's t test using Welch's correction for unequal variances was used.

409

410

411

412

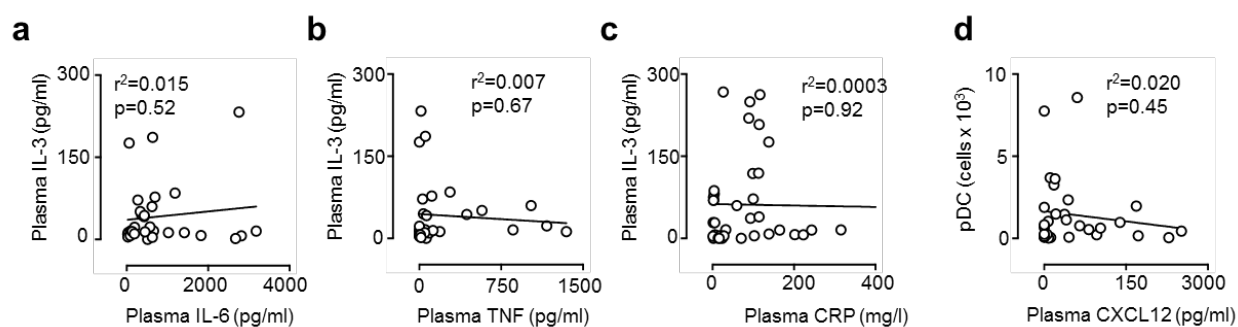
413

414

415

416

417



418

419 **Extended Data Fig. 4. Plasma IL-3 levels do not correlate with plasma IL-6, TNF, CRP**

420 **levels and circulating pDCs. a-c, Correlation between plasma IL-3 levels and plasma IL-6**

421 **(a), TNF (b) and CRP (c) levels in SARS-CoV-2<sup>+</sup> patients. n=32. d, Correlation between**

422 **plasma CXCL12 levels and the amount of circulating pDCs in SARS-CoV-2<sup>+</sup> patients. n=32.**

423

424

425

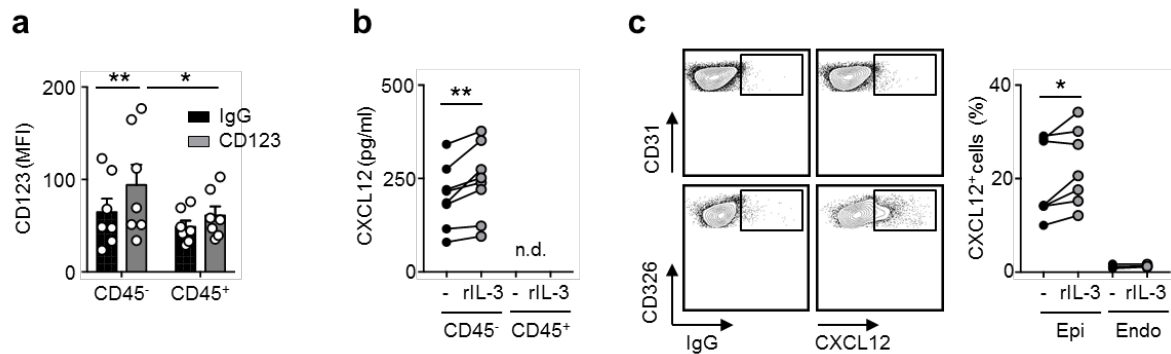
426

427

428

429

430



431

432 **Extended Data Fig. 5. Interleukin-3 induces CXCL12 in lung epithelial cells.** **a**, CD123

433 expression (MFI) on the surface of CD45<sup>-</sup> and CD45<sup>+</sup> cells from the lungs of naive mice. n=8.

434 **b**, Level of CXCL12 in the supernatant of CD45<sup>-</sup> or CD45<sup>+</sup> cells purified from the lungs of

435 naive mice 24 h after *ex vivo* stimulation with or without IL-3. n=8. **c**, Representative dot plot

436 (left) and percentage (right) of CXCL12<sup>+</sup> epithelial or endothelial cells in the lungs of mice 24

437 h after *ex vivo* stimulation with or without IL-3. n=7. Data are mean  $\pm$  s.e.m., \*P < 0.05, \*\*P

438 < 0.01, \*\*\*P < 0.001, paired, 2-tailed Student's t test and unpaired, 2-tailed Student's t test

439 using Welch's correction for unequal variances was used.

440

441

442

443

444 **Extended Data Table 1: Minimum p-value approach for IL-3 (n=64).**

445

| <b>IL-3-value (pg/ml)</b> | <b>p-value (LogRank)</b> | <b>IL-3</b> | <b>N</b>  | <b>60-days survival</b> |
|---------------------------|--------------------------|-------------|-----------|-------------------------|
| <b>50</b>                 | 0.111                    | Low         | 53        | 79.2%                   |
|                           |                          | High        | 11        | 100%                    |
| <b>30</b>                 | 0.064                    | Low         | 50        | 78.0%                   |
|                           |                          | High        | 14        | 100%                    |
| <b>25</b>                 | 0.034                    | Low         | 47        | 76.6%                   |
|                           |                          | High        | 17        | 100%                    |
| <b>20</b>                 | <b>0.027</b>             | <b>Low</b>  | <b>46</b> | <b>76.1%</b>            |
|                           |                          | <b>High</b> | <b>18</b> | <b>100%</b>             |
| <b>15</b>                 | 0.822                    | Low         | 39        | 82.1%                   |
|                           |                          | High        | 25        | 84.0%                   |
| <b>10</b>                 | 0.503                    | Low         | 35        | 85.7%                   |
|                           |                          | High        | 29        | 79.3%                   |
| <b>5</b>                  | 0.397                    | Low         | 24        | 87.5%                   |
|                           |                          | High        | 40        | 80.0%                   |

446

447

448 **Extended Data Table 2: Multivariate analysis of the impact of different risk factors on**  
449 **mortality following SARS-CoV-2-infection (n=64).**

450

|                             | Univariate   | Multivariate |               |              |
|-----------------------------|--------------|--------------|---------------|--------------|
|                             | p-value      | HR           | CI            | p-value      |
| <b>Age ≥ 65 years</b>       | <b>0.042</b> | -            | -             | 0.157        |
| <b>Gender</b>               | 1.000        |              |               |              |
| <b>CRP &lt; 140 mg/l*</b>   | <b>0.001</b> | 0.102        | 0.019 – 0.552 | <b>0.002</b> |
| <b>IL-3 ≥ 20 pg/ml**</b>    | <b>0.026</b> | 0.000        | 0.000         | <b>0.026</b> |
| <b>CXCL12 ≥ 10 pg/ml*</b>   | 0.322        |              |               |              |
| <b>Invasive ventilation</b> | <b>0.045</b> | -            | -             | 0.468        |
| <b>ECMO</b>                 | 0.134        |              |               |              |

451

452 \*cutoff was determined using p-value approach; bold values are significant (p < 0.05).

453 \*\*HR and CI are “0.000” because no patient died when IL-3 ≥20 pg/ml.

454

455

456

457 **Extended Data Table 3: Risk to die from SARS-CoV-2 according to risk groups**

458

| <b>Risk to die</b>  | <b>Mortality</b> | <b>Mortality</b> | <b>OR</b> | <b>95%-CI</b>   |
|---------------------|------------------|------------------|-----------|-----------------|
| <b>low</b>          | 0 / 10 (0%)      | 1 / 32 (3%)      | -         | -               |
| <b>intermediate</b> | 1 / 22 (5%)      | 10 / 32 (31%)    | 14.091    | 1.680 – 118.218 |
| <b>high</b>         | 10 / 32 (31%)    |                  |           |                 |

459

460 Low (IL-3  $\geq$ 20 pg/ml and age <65 years) and intermediate (IL-3 <20 pg/ml and age <65 years  
461 or IL-3  $\geq$ 20 pg/ml and age  $\geq$ 65 years) vs. high (IL-3 <20 pg/ml and age  $\geq$ 65 years).

462

463

464

465

466

467

468

469

470

471

472

473

474

475

476

477

478

479

480

481 **Extended Data Table 4: Baseline data of patients scheduled for elective bronchoalveolar**  
482 **lavage.**

483

---

**Baseline data of the BAL group (n=13)**

---

**Demographic data**

|          |                    |
|----------|--------------------|
| Age, y   | 61.0 ( $\pm$ 13.8) |
| Male sex | 10 (76.9%)         |

**Localization of the BAL**

|                   |           |
|-------------------|-----------|
| Right upper lobe  | 5 (38.5%) |
| Right middle lobe | 2 (15.4%) |
| Right lower lobe  | 2 (15.4%) |
| Left upper lobe   | 4 (30.8%) |
| Left lower lobe   | 0 (0%)    |

**Main diagnosis**

|                         |            |
|-------------------------|------------|
| Primary respiratory     | 10 (76.9%) |
| Non-inflammatory        | 4 (40%)    |
| Inflammatory            | 6 (60%)    |
| Primary non-respiratory | 2 (15.4%)  |
| Unknown                 | 1 (7.7%)   |

---

484 Data is presented as the number (%) or the mean ( $\pm$  standard deviation).

485



486 **Extended Data Table 5: Baseline data of patients scheduled for elective thoracic surgery**  
487 **to obtain lung tissue.**

488

---

**Baseline data of the lung tissue specimens (n=15)**

---

**Demographic data**

|          |                   |
|----------|-------------------|
| Age, y   | 61.9 ( $\pm$ 7.6) |
| Male sex | 7 (46.7%)         |

**Localization of lung tissue**

|                   |           |
|-------------------|-----------|
| Right upper lobe  | 7 (46.7%) |
| Right middle lobe | 0 (0.0%)  |
| Right lower lobe  | 3 (20.0%) |
| Left upper lobe   | 1 (6.7%)  |
| Left lower lobe   | 4 (26.7%) |

**Main diagnosis**

|                         |            |
|-------------------------|------------|
| Primary respiratory     | 13 (86.7%) |
| Non-inflammatory        | 11 (84.6%) |
| Inflammatory            | 2 (15.4%)  |
| Primary non-respiratory | 2 (13.3%)  |

---

489 Data is presented as the number (%) or the mean ( $\pm$  standard deviation).

490

491

492

493

494

495

496

497

498

499 **Extended Data Table 6: Mouse primer**

500

|               |                               |                                 |
|---------------|-------------------------------|---------------------------------|
| <i>Hprt</i>   | 5'-GTTCTTTGCTGACCTGCTGGAT-3'  | 5'-CCCCGTTGACTGATCATTACAG-3'    |
| <i>Ccl2</i>   | 5'-CCACTCACCTGCTGCTACTCATT-3' | 5'-TTCCTTCTTGGGGTCAGCACAGAC-3'  |
| <i>Cxcl9</i>  | 5'-AGCAGTGTGGAGTTCGAGGAAC-3'  | 5'-AGGGATTGTAGTGGATCGTGC-3'     |
| <i>Ccl21</i>  | 5'-AGAACCTGATGCGCCGC-3'       | 5'-GGCTGTGTCTGTTTCAGTTCTCTTG-3' |
| <i>Cxcl12</i> | 5'-CTGTGCCCTTCAGATTGTTG-3'    | 5'-TTTCTTCTCTGCGCCCCTT-3'       |

501

502

503

504

505

506

507

508

509

510

511

512

513